GEOPHYSICS, VOL. 73, NO. 4 (JULY-AUGUST 2008); P. D53–D62, 8 FIGS., 1 TABLE.
10.1190/1.2938036

Rational interpolation of qP-traveltimes for semblance-based anisotropy estimation in layered VTI media

Huub Douma[1] and Mirko van der Baan[2]

ABSTRACT

The τ-p domain is the natural domain for anisotropy parameter estimation in horizontally layered media. The need to transform the data to the τ-p domain or to pick traveltimes in the t-x domain is, however, a practical disadvantage. To overcome this, we combine τ-p-derived traveltimes and offsets in horizontally layered transversely isotropic media with a vertical symmetry axis (VTI) with a rational interpolation procedure applied in the t-x domain. This combination results in an accurate and efficient t-x-based semblance analysis for anisotropy parameter estimation from the moveout of qP-waves in horizontally layered VTI media. The semblance analysis is applied to the moveout to search directly for the interval values of the relevant parameters. To achieve this, the method is applied in a layer-stripping fashion. We demonstrate the method using synthetic data examples and show that it is robust in the presence of random noise and moderate statics.

INTRODUCTION

In the past two decades, seismic processing has gradually developed to allow for estimation of anisotropy parameters from seismic data. In the presence of anisotropy, the moveout of qP-waves in horizontally layered media as observed in common-midpoint (CMP) gathers deviates from being hyperbolic. It is common practice to get (initial) estimates of the relevant anisotropic parameters by ascribing the nonhyperbolic character of the moveout to the presence of anisotropy. This method originated with the work of Hake et al. (1984), who presents a three-term Taylor expansion to describe the moveout in a CMP gather acquired over a horizontally layered transversely isotropic (TI) medium.

Tsvankin and Thomsen (1994) and Alkhalifah and Tsvankin (1995) present an improved rational approximation that provided better accuracy at longer offsets, but many authors subsequently point out the lack of accuracy at intermediate offsets (e.g., Zhang and Uren, 2001; Van der Baan and Kendall, 2002; Stovas and Ursin, 2004; Douma and Calvert, 2006). This observation has led to several other methods, such as the stationary-phase method (Alkhalifah, 2000), the τ-p method (Van der Baan and Kendall, 2002; Van der Baan, 2004), the shifted-hyperbola approach (e.g., Fomel, 2004), continued-fraction approaches (e.g., Ursin and Stovas, 2006), and a rational-interpolation method (Douma and Calvert, 2006).

The τ-p transform is the natural domain for anisotropy parameter estimation in layered media (Hake, 1986; Van der Baan and Kendall, 2002) because the horizontal slowness is preserved upon propagation through such media. Because the τ-p transform is a plane-wave decomposition, the relevant velocity is the phase velocity instead of the group velocity. The latter velocity is mathematically more complex and often follows from approximations to already-approximated phase velocities. Hence, anisotropy parameter estimation in the τ-p domain renders the extra approximation for the group velocity redundant, leading to more accurate estimates of the relevant parameters. It has an additional advantage in that the inversion algorithm is explicitly formulated in terms of the normal-moveout (NMO) velocity V_{nmo} and the anisotropy parameter η, the parameters most often sought for in P-wave traveltime inversion from surface seismics alone. Finally, triplications in the t-x domain are unfolded in the τ-p domain, allowing anisotropy parameter estimation when the wavefront contains cusps (Alkhalifah and de Hoop, 2005).

Besides these benefits, τ-p-domain inversion techniques have a main practical disadvantage: either the CMP gathers need to be transformed to the τ-p domain or the $t(x)$ moveout curves need to be picked in the t-x domain and subsequently transformed to the τ-p domain. Because most interpreters have more experience viewing data in the t-x domain, Van der Baan and Kendall (2002) recommend the latter option. To make this picking more robust, they propose fitting an analytic curve to the picked traveltimes and transforming the

Manuscript received by the Editor 9 October 2007; revised manuscript received 12 December 2007; published online 8 July 2008.
[1]Formerly Colorado School of Mines, Department of Geophysics, Center for Wave Phenomena, Golden, Colorado, U.S.A; presently Princeton University, Department of Geosciences, Princeton, New Jersey, U.S.A. E-mail: hdouma@princeton.edu.
[2]University of Leeds, School of Earth and Environment: Earth Sciences, Leeds, U. K. E-mail: m.van-der-baan@see.leeds.ac.uk.

latter to the τ-p domain. However, traveltime picking is a cumbersome and time-consuming exercise prone to error. Moreover, the accuracy of the estimated anisotropy to some extent depends on the ability of the analytic curve to describe the actual traveltimes accurately.

Direct application of the τ-p inversion technique in the t-x domain (e.g., using a semblance-based approach) is needlessly cumbersome and inefficient because it entails solving a two-point ray-tracing problem for every recorded offset (i.e., trace). In this paper, we develop an efficient semblance-based approach for anisotropy parameter estimation based on rational interpolation in the t-x domain while maintaining the accuracy of the τ-p domain inversion technique. The rational interpolation ensures that we have to solve a two-point ray-tracing problem for few offsets (here, four) only.

Douma and Calvert (2006) present an efficient rational-interpolation method for qP-waves in the t-x domain that combines accurate moveout correction with unbiased parameter estimation up to arbitrary levels of anellipticity and large offset-to-depth ratios (x/z). Their method is semblance based and thus generally less cumbersome and probably more robust than manual picking of traveltimes, as done in τ-p-domain methods. However, the method of Douma and Calvert (2006) is restricted to a single horizontal transversely isotropic layer with a vertical symmetry axis (VTI). In this work, we extend their method to create a semblance-based approach for anisotropy parameter estimation in horizontally layered VTI media in the t-x domain. Our method allows the estimation of interval values of the anellipticity parameter η and (zero-dip) normal-moveout velocity V_{nmo} from the observed nonhyperbolic moveout of qP-waves without using a Dix-type layer-stripping procedure (Dix, 1955). Such a procedure is valid for small offset-to-depth ratios only, whereas our method is accurate for large offset-to-depth ratios.

The expressions we derive for the traveltimes and offsets are explicit in the interval values of η and V_{nmo} and the horizontal slowness. They allow efficient computation of the support points for the rational interpolation. Beyond that, rational interpolation obtains accurate traveltime interpolants with only a few (here, five) support points. Therefore, the method is both accurate and efficient. The traveltime and offset expressions are derived based on the acoustic approximation of Alkhalifah (1998).

The organization of this paper is as follows: First, we develop explicit expressions for the traveltimes and offsets of pure-mode qP-reflected waves in layered VTI media as a function of the interval values of η, V_{nmo}, the interval zero-offset two-way traveltime Δt_0, and the horizontal slowness. These expressions allow fast computation of the support points of the interpolation. We then proceed to present the rational-interpolation-based procedure to calculate the moveout, and explain its use in the semblance-based interval-parameter estimation of η and V_{nmo}. Finally, we test the method using synthetic data examples with and without noise.

ANISOTROPY PARAMETER ESTIMATION IN LAYERED VTI MEDIA

Nonhyperbolic moveout of qP-waves as a function of horizontal slowness

The τ-p transform relates traveltime t and offset x to intercept time τ and horizontal slowness p by

$$t = px + \tau . \tag{1}$$

The total intercept time τ for a reflected wave in a horizontally layered medium with a horizontal symmetry plane is a linear combination of the interval zero-offset traveltimes Δt_0^i, the vertical phase-velocity v_0^i, and the vertical slowness q_i in each layer i (Hake, 1986; Van der Baan and Kendall, 2002). It is given by

$$\tau = \sum_i \Delta t_0^i v_0^i q_i . \tag{2}$$

Because horizontally layered VTI media have a horizontal plane of symmetry, the latter expression holds for qP-waves as well as for qSV- and qSH-waves.

Traveltimes of qP-waves in TI media depend mainly on V_{nmo} and η (Alkhalifah and Tsvankin, 1995). The vertical shear-wave phase velocity V_{S0} has negligible influence on these traveltimes (Tsvankin and Thomsen, 1994; Tsvankin, 1996; Alkhalifah, 1998). This enables Alkhalifah (1998) to derive an approximate relation for the vertical slowness q of qP-waves in TI media in terms of V_{nmo} and η by setting $V_{\mathrm{S0}} = 0$. It is given by

$$V_{P0}^2 q^2 = 1 - \frac{1 - p^2 V_{\mathrm{nmo}}^2}{1 - 2\eta p^2 V_{\mathrm{nmo}}^2}, \tag{3}$$

where V_{P0} is the vertical qP-wave phase velocity. Setting $V_{\mathrm{S0}} = 0$ is often referred to as the acoustic approximation of Alkhalifah (1998); Grechka and Tsvankin (1998) show that the horizontal velocity $V_{\mathrm{hor}} = V_{\mathrm{nmo}}\sqrt{1 + 2\eta}$ is better constrained in a semblance-based moveout analysis than η. In anticipation of a semblance-based parameter estimation, we rewrite equation 3 in terms of V_{hor} and V_{nmo}, and substitute the result into expression 2, yielding

$$\tau = \sum_i \Delta t_0^i \sqrt{\frac{1 - p^2 (V_{\mathrm{hor}}^i)^2}{1 - p^2[(V_{\mathrm{hor}}^i)^2 - (V_{\mathrm{nmo}}^i)^2]}}, \tag{4}$$

with V_{hor}^i and V_{nmo}^i the horizontal and NMO velocities in layer i, respectively.

To create a t-x semblance analysis, we need to know the traveltime for each recorded offset x. It follows from the definition of the τ-p transform 1 that

$$x = -\left(\frac{\partial \tau}{\partial p}\right). \tag{5}$$

Inserting equation 4 in this expression yields the offset x as a function of p, Δt_0^i, V_{hor}^i, and V_{nmo}^i:

$$x = \sum_i \Delta t_0^i \left(\frac{\dfrac{p (V_{\mathrm{nmo}}^i)^2}{A^i(p)^{3/2}\sqrt{1 - p^2 (V_{\mathrm{hor}}^i)^2}}}{A^i(p) = 1 - p^2[(V_{\mathrm{hor}}^i)^2 - (V_{\mathrm{nmo}}^i)^2]} \right). \tag{6}$$

Combining equations 1, 4, and 6 then gives the traveltime t associated with this offset x as a function of p, Δt_0^i, V_{hor}^i, and V_{nmo}^i:

$$t = \sum_i \Delta t_0^i \left(\frac{p^2 (V_{\mathrm{nmo}}^i)^2 / A^i(p) + [1 - p^2 (V_{\mathrm{hor}}^i)^2]}{\sqrt{[1 - p^2 (V_{\mathrm{hor}}^i)^2] A^i(p)}} \right). \tag{7}$$

Equations 6 and 7 are explicit in the horizontal slowness p, whereas for a t-x-based semblance analysis we require traveltimes for each offset acquired in the field. However, the p-value that corresponds to a certain offset x in equation 6 can be found using a numerical method such as the bisection approach because expression 6 is single val-

ued and monotonically increasing with increasing p-values. Using this p-value in equation 7 gives the associated traveltime. In principle, this could be done for every offset in a CMP gather. However, a more elegant and computationally less demanding procedure is available using the rational interpolation approach of Douma and Calvert (2006).

Rational interpolation

The particular choice of Douma and Calvert (2006) to use a rational interpolation was motivated by the original improvement in accuracy when Tsvankin and Thomsen (1994) replaced the original three-term Taylor approximation of Hake et al. (1984) with a rational approximation. This approximation was later rewritten in terms of V_{nmo} and η (or V_{hor}) by Alkhalifah and Tsvankin (1995). Throughout the remainder of this work, we refer to this approximation as the Alkhalifah-Thomsen-Tsvankin (ATT) approximation.

Recognizing the need for improved accuracy beyond the ATT approximation, Douma and Calvert (2006) replace the rational approximation with a rational interpolation that provides accuracy at offsets where it is needed, i.e., at offsets acquired in the field. In addition, Douma and Calvert (2006) show that because of the improved accuracy, the systematic error in the estimated values of η, present in the values obtained with the ATT approximation, are removed. Here, we extend their method to horizontally layered VTI media to allow estimation of the interval values of V_{hor} and V_{nmo} by interpolating offsets and associated traveltimes from equations 6 and 7, respectively, obtained from a few horizontal slownesses. Because we are dealing with qP-waves only, interpolation can be done in the t-x domain because no cusps can occur on qP-wavefronts due to the convexity of the slowness surface of such waves.

A rational approximation to a function $T(X)$ is generally written as (e.g., Stoer and Bulirsch, 1993, p. 58–96)

$$T(X) \approx \frac{N_L(X)}{D_M(X)} = \frac{n_0 + n_1 X + \cdots + n_L X^L}{1 + d_1 X + \cdots + d_M X^M}, \tag{8}$$

with $N_L(X)$ a polynomial of order L and $D_M(X)$ a polynomial of order M. We denote such an approximation as $[L/M]$. This rational approximation is fully determined by the $L + M + 1$ unknown coefficients $n_i (i = 0, 1, \ldots, L)$ and d_i $(i = 1, \ldots, M)$ that satisfy

$$T(X_i) = \frac{N_L(X_i)}{D_M(X_i)} = T_i. \tag{9}$$

It follows then that the coefficients must satisfy the linear system

$$N_L(X_i) - T_i D_M(X_i) = 0. \tag{10}$$

To find the unknown coefficients n_i and d_i, Douma and Calvert (2006) explicitly solve this linear system (see their Appendix A). Alternatively, the rational approximant $N_L(X)/D_M(X)$ can be written as a Thiele continued fraction (Stoer and Bulirsch, 1993, p. 63–67), given by

$$\frac{N_L(X)}{D_M(X)} = n_0 + \frac{X - X_0}{\rho(X_0,X_1) +} \frac{X - X_1}{\rho(X_0,X_1,X_2) - \rho(X_0) +} \cdots \times \frac{X - X_{M+L-1}}{\rho(X_0, \ldots, X_{M+L}) - \rho(X_0, \ldots, X_{M+L-2})}, \tag{11}$$

where we define the notation

$$\frac{a}{b+} \frac{c}{d} = \frac{a}{b + c/d}$$

and where the reciprocal differences ρ are defined by

$$\rho(X_i) = T_i, \tag{12}$$

$$\rho(X_i, X_k) = \frac{X_i - X_k}{T_i - T_k}, \tag{13}$$

$$\rho(X_i, X_{i+1}, \ldots, X_{i+k}) = \frac{X_i - X_{i+k}}{\rho(X_i, \ldots, X_{i+k-1}) - \rho(X_{i+1}, \ldots, X_{i+k})} + \rho(X_{i+1}, \ldots, X_{i+k-1}). \tag{14}$$

In this work, we use the same order of rational interpolation that Douma and Calvert (2006) use, i.e., a [2/2] rational interpolation, because they show that this order of interpolation (at least for a single horizontal homogeneous VTI layer) provides high accuracy in traveltimes up to $x/z = 8$. Setting $L = M = 2$ in equation 11 gives the desired Thiele continued-fraction interpolation for nonhyperbolic moveout of qP-waves in VTI media, i.e.,

$$T(X) \approx \frac{N_2(X)}{D_2(X)} = T_0 + \frac{X}{\rho(X_0,X_1) +} \frac{X - X_1}{\rho(X_0, \ldots, X_2) - T_0 +} \frac{X - X_2}{\rho(X_0, \ldots, X_3) - \rho(X_0,X_1) +} \frac{X - X_3}{\rho(X_0, \ldots, X_4) - \rho(X_0, \ldots, X_2)}, \tag{15}$$

where we use $\rho(X_0) = T_0$ and anticipate treating the zero-offset support point (X_0, T_0) as a parameter with $X_0 = 0$, giving $n_0 = T_0$ (see equation 8). Just as Douma and Calvert (2006) do, we interpolate support points (X_i, T_i), with X denoting squared offset and T squared traveltimes.

Equation 15 provides the squared traveltimes $T(X)$ at arbitrary squared offsets X away from the support points (X_i, T_i). The reciprocal differences ρ are computed directly from the support points using equations 12–14. Only four (instead of $L + M + 1 = 5$) support points are needed for [2/2] rational interpolation because $T_0 = t_0^2 = (\Sigma_{i=1}^n t_0^i)^2$ is treated as a parameter with $X_0 = x_0^2 = 0$. The need to calculate so few support points makes the method efficient.

Nothing prevents the numerator $N_L(X_i)$ and denominator $D_M(X_i)$ in equation 8 from having common roots $(X - X_i)$. In this case, equation 10 is still satisfied, but the linear system it represents cannot be solved for the unknown interpolation coefficients n_i and d_i. However, such nonsolvability is a matter of degeneracy only (Stoer and Bulirsch, 1993, p. 61–62). In practice, degeneracy can be overcome by adding arbitrary small perturbations to the support points (for example, on the order of $O[10^{-1}]$ms or smaller for traveltimes and/or $O[10^{-1}]$m or smaller for offsets).

In the case of [2/2] rational interpolation, degeneracy occurs for purely hyperbolic moveout when squared offset and squared traveltime are interpolated (Douma and Calvert, 2006), as shown in Ap-

pendix A). Indeed, we overcome this degeneracy throughout our work by noise injection. In principle, this degeneracy could be avoided by interpolating the traveltimes as a function of offset instead of squared traveltimes as a function of squared offset. However, we found that interpolating squared traveltimes as a function of squared offsets leads to more accurate traveltimes than interpolation of traveltime t as a function of offset x. The ATT approximation uses squared traveltime and squared offset also.

Semblance-based interval-parameter estimation

To perform semblance analysis in the t-x domain, we must be able to compute the traveltime for each offset acquired in the field for a particular t_0 and a particular combination of V_{hor} and V_{nmo}. For example, we might aim to perform a semblance scan as a function of the interval horizontal and NMO velocities for the nth layer specified by a specific interval zero-offset traveltime t_0^n. To do this, we assume the values of t_0^i, V_{hor}^i, and V_{nmo}^i for $i = 1, \ldots, n-1$ are known, e.g., by applying our approach in a layer-stripping fashion.

First, a range of interval horizontal and NMO velocities V_{hor}^n and V_{nmo}^n is specified. Next, for each particular combination of V_{hor}^n and V_{nmo}^n, four user-specified x/z values $k_j (j = 1, \ldots, 4)$ are converted to target offsets $\tilde{x}_j = (k_j/2)\Sigma_{i=1}^n V_{\text{nmo}}^i t_0^i$. We must then find the associated horizontal slownesses p_j that correspond to offsets close to the target offsets $\tilde{x}_j$ (within an accuracy of approximately 100 m). We do this using a bisection approach applied to equation 6. We are thus, in essence, building a simplified two-point ray-tracing algorithm for horizontally layered VTI media.

Once the slowness values p_j are found, they are used in equations 6 and 7 to find the squared offsets $X_j = x_j^2$ and traveltimes $T_j = t_j^2$ that form the support points for the rational interpolation. Using the obtained values of X_j and T_j in equations 12–14 to calculate the reciprocal differences ρ, we then find the desired interpolation curve $T(X)$ from equation 15, which gives the squared traveltime T as a function of any squared offset X. These traveltime curves allow a semblance analysis as a function of the interval parameters V_{hor}^n and V_{nmo}^n for each layer n. As an alternative to bisection, ray shooting can be considered to compute the desired support points. In this approach, offsets for a range of slowness values are computed, and the ones closest to the desired ones are extracted to act as the support offsets and traveltimes.

Because the offset and traveltime equations 6 and 7 are expressed in terms of the interval velocities V_{hor}^i and V_{nmo}^i, a semblance-based global inversion can in principle be set up to determine the values of V_{hor}^i and V_{nmo}^i for all layers at the same time. More practically, the inversion can be done in a layer-stripping fashion. However, such approaches are not always desirable because of the trade-off between V_{hor}^i and V_{nmo}^i for limited-offset acquisition geometries. Alternatively, once the layer of interest is determined, the overburden can be modeled as a single layer for which the effective values of V_{hor} and V_{nmo} are determined. Subsequently, an interval semblance analysis using the approach outlined above provides the interval estimates V_{hor}^i and V_{nmo}^i of the target layer. However, in this approach, the estimated values of V_{hor}^i and V_{nmo}^i will to some extent depend on the ability to represent the traveltime-curve of the overburden using a single effective horizontal VTI layer.

In general, interval parameter estimation is inherently more difficult than estimation of effective values, and substantial x/z values must be present for the target horizon (larger than about 2 or 2.5; Alkhalifah, 1997) for anisotropy parameter estimation to succeed. Our approach obviously specializes in the case of a single horizontal VTI layer treated by Douma and Calvert (2006). For this special case, their highly efficient tabulated approach is preferred because it does not need to solve equation 6 to find the p value associated with each target offset $\tilde{x}_j$.

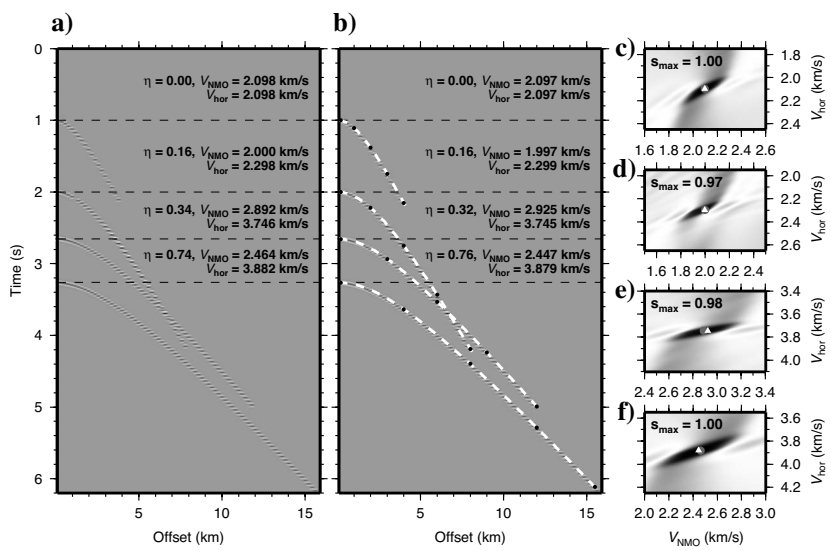

Figure 1. CMP gather with qP-reflections for a four-layer model generated using ray tracing (see Table 1 for parameters); maximum $x/z = 4$. The layers are outlined by dashed lines, and the true values of η, V_{hor}, and V_{nmo} are indicated. (b) As (a) but with estimated values of η, V_{hor}, and V_{nmo} indicated together with their associated traveltimes (dashed white lines). The support points are marked by the black dots. (c-f) Semblance scans as a function of the interval values of V_{hor} and V_{nmo} for (c-f) layers 1–4, respectively. Gray circles: true interval values V_{hor}^i, and V_{nmo}^i; white triangles: estimated interval values. All interval values have been estimated accurately, and the corresponding traveltime predictions are accurate as indicated by the high semblance maxima ($s_{\max} \approx 1$).

SYNTHETIC DATA EXAMPLES

The same four-layer model as in Douma and Calvert (2006) is used to demonstrate the accuracy of the inversion approach to estimate interval parameters (Figure 1a). The model parameters are given in Table 1; the values of η, V_{hor}, and V_{nmo} are also listed in Figure 1a for each layer.

The top layer is elliptically anisotropic, i.e., $\eta = 0$, but the remaining layers have subsequently increasing levels of anellipticity. The values of V_{nmo}, V_{hor}, and η for the second layer are also used in Figures 1 and 2 of Grechka and Tsvankin (1998) and correspond to values observed in field data (Alkhalifah et al., 1996). The level of anellipticity for the third layer ($\eta = 0.34$) can be considered high, whereas the anellipticity in the fourth layer ($\eta = 0.74$) is certainly extreme. The model parameters for the third and fourth layer are not physically unfeasible but correspond, respectively, to a shale under zero confining pressure and to Green River shale (see Table 1 in Thomsen (1986) for these two cases).

The dominant frequency of the events is 20 Hz, and the maximum offset-to-depth ratio $x/z = 4$ for all events. No phase or amplitude variations were modeled for any events in Figure

1a to prevent the semblance results suffering from such variations with offset — a known shortcoming of semblance-based analysis (Sarkar et al., 2002). At 7-km offset and 3.8-s traveltime, there is a variation in amplitude and phase caused by crossing the reflected events from the second and third layer.

Figure 1c-f shows the semblance scans for the first through the fourth reflections in Figure 1a as a function of the interval horizontal and NMO velocities $V^i_{\rm hor}$ and $V^i_{\rm nmo}$. The semblance scans are obtained with a layer-stripping approach. The maximum-semblance location is indicated by the white triangle; the location corresponding to the true model values of $V^i_{\rm hor}$ and $V^i_{\rm nmo}$ is indicated by the gray circle. The semblance contours are centered around the true model parameters. The close proximity of the white triangle and the gray circle indicates the retrieved velocities at the position of maximum semblance (Figure 1b) are in excellent agreement with the true values (Figure 1a). The accuracy of the inversion is also confirmed by the high semblance maxima ($s_{\rm max} \approx 1$), even for the high offset-to-depth ratios and extreme levels of anellipticity involved.

On the other hand, the trade-off between $V^i_{\rm hor}$ and $V^i_{\rm nmo}$ is weak only because of the relatively large offset-to-depth ratio $x/z = 4$. The semblance values for the second and third layer are slightly less than one because the reflections are crossing, causing both phase and amplitude changes that affect the maximum-semblance value. As the ratio of the interval traveltime to the total traveltime decreases, the semblance contours become wider; as a result, the parameters become less well resolved. Figure 1b shows the traveltime curves, calculated using the recovered values of $V^i_{\rm hor}$ and $V^i_{\rm nmo}$, superimposed on the true moveout curves. Discrepancies are negligible, again demonstrating the high accuracy of our method.

We compare our results with those obtained using the technique of Grechka and Tsvankin (1998) to find the interval values $V^i_{\rm hor}$ and $V^i_{\rm nmo}$ from the effective values of $V_{\rm nmo}$ and $V_{\rm hor}$ using the ATT approximation. We refer to this method as the GT method throughout the remainder of this work.

Figure 2a-c shows the estimated interval values $V^i_{\rm nmo}$, $V^i_{\rm hor}$, and η_i, respectively, obtained using the GT method, for all four layers in our synthetic CMP gather (Figure 1a) and as a function of the maximum x/z. Clearly, the GT method provides an accurate estimate of $V^i_{\rm nmo}$ at least up to $x/z = 4$ for all layers except the third. The estimated values of $V^i_{\rm hor}$, on the other hand, are accurate only for the first two layers but are clearly biased at higher levels of anellipticity and vary with the maximum x/z used. That is, the estimated $V^i_{\rm hor}$ contain a systematic error for higher levels of anellipticity. This systematic error at higher levels of anellipticity is caused by the inaccuracy of the ATT approximation pointed out by many authors (e.g., Zhang and Uren, 2001; Van der Baan and Kendall, 2002; Stovas and Ursin, 2004; Douma and Calvert, 2006). As a result, the values of η_i are strongly biased for all but the first two layers and are dependent on the maximum x/z values used.

The same analysis using our method shows that the estimated values of $V^i_{\rm nmo}$, $V^i_{\rm hor}$, and η_i have negligible systematic errors independent of the maximum x/z used (Figure 2d-f) for all layers and thus for arbitrary levels of anellipticity. We mention that the estimates of $V_{\rm nmo}$ (and thus η) for the third layer at $x/z > 2.5$ show a small deviation from the true value. This is caused by the crossing of the events from layers two and three at $x \approx 7$ km, which creates a variation in phase and amplitude that is known to affect semblance-based parameter estimation (Sarkar et al., 2002). This is also the probable cause of the error in the estimated values of $V^i_{\rm nmo}$ for this layer using the GT method (see Figure 2).

Figure 2 implies the improved accuracy of our method over the GT method for the noiseless example. However, it cannot be determined whether the differences between the estimated parameter values for both methods are significant without considering the uncertainty in the estimated values of $V^i_{\rm hor}$ and $V^i_{\rm nmo}$. We demonstrate that

Table 1. Model parameters used in ray tracing to determine traveltimes from a layered model, where h is the layer thickness and ϵ and δ are the familiar Thomsen parameters (Thomsen, 1986). The associated events are shown in Figure 1a.

Layer	h (m)	$V_{\rm nmo}$ (m/s)	$V_{\rm hor}$ (m/s)	η	V_{P0} (m/s)	V_{S0} (m/s)	ϵ	δ
1	1000	2098	2098	0.00	2000	300	0.050	0.05
2	2000	2000	2298	0.16	2000	300	0.160	0.00
3	3000	2892	3746	0.34	3048	300	0.255	− 0.05
4	4000	2464	3882	0.74	3292	300	0.195	− 0.22

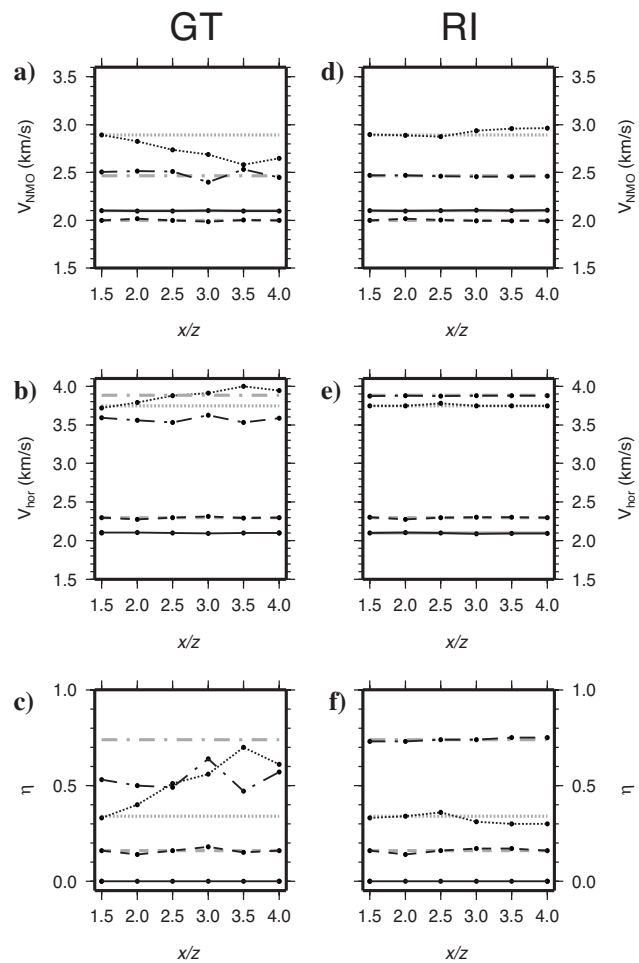

Figure 2. Estimated values (black) of (a) $V^i_{\rm nmo}$, (b) $V^i_{\rm hor}$, and (c) η_i for layers 1 (drawn), 2 (dashed), 3 (dotted), and 4 (dash-dotted), using the GT method. The gray curves indicate the true values. (d-f) As (a-c) but using our method based on rational interpolation. The method obtains unbiased estimates independent of the maximum offset-to-depth ratio.

these differences are indeed important by plotting the estimated parameters for the third layer for both methods in the semblance scans that are calculated using our method (Figure 3). The values estimated using the GT method are outside the main contours of the semblance scans for $x/z > 2.5$. Therefore, the differences between both methods are indeed significant, at least for $x/z > 2.5$, i.e., at x/z ratios that are crucial for robust interval parameter estimation (Alkhalifah, 1997).

The quality of the horizontal and NMO velocity estimates can also be judged by their ability to flatten the events in Figure 1a. Figure 4 shows flattened traveltime curves using parameter estimates obtained using (1) the ATT approximation; (2) rational interpolation while treating the overburden as a single horizontal VTI layer, i.e., effective rational interpolation; and (3) the interval-semblance method. All methods were tested for a range of maximum offset-to-depth ratios: $x/z = 2$ (blue), $x/z = 3$ (red), and $x/z = 4$ (black).

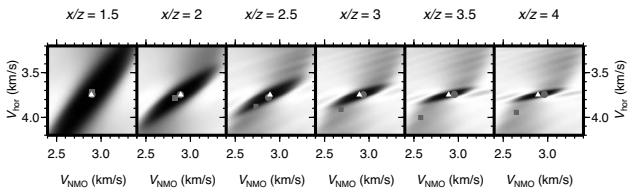

Figure 3. Semblance scan for layer 3, calculated using the presented method based on rational interpolation, as a function of x/z. Gray circles: true interval horizontal and NMO velocities in layer 3; white triangles: maximum semblance location; gray squares: estimated values of interval horizontal and NMO velocities using the GT method. True values and the maximum semblance location are nearly coincident, indicating the accuracy of our method. The retrieved values using the GT approach are well outside the semblance contours for $x/z > 2.5$, that is, once nonhyperbolic moveout becomes noticeable. This indicates the GT estimates are well outside the uncertainties associated with our estimates for $x/z > 2.5$.

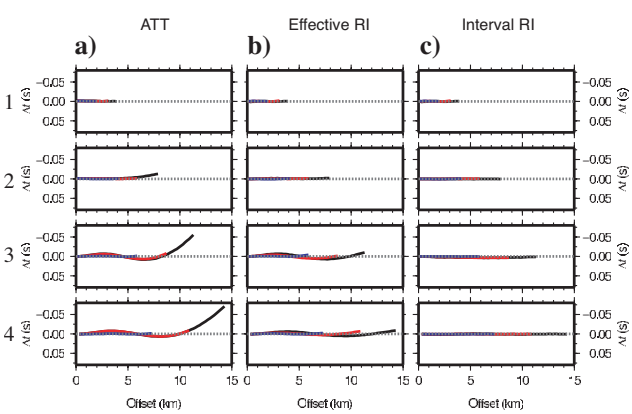

Figure 4. Residual moveout for all four events with (a) the ATT approximation, (b) single-layer (or effective) rational interpolation, and (c) our method using rational interpolation for layered VTI media for maximum $x/z = 2$ (blue), $x/z = 3$ (red), and $x/z = 4$ (black). Our method clearly outperforms the ATT approximation for large offset-to-depth ratios (at least $x/z \leq 4$) and up to extreme levels of anellipticity. Treating the overburden as a single effective layer develops observable residual moveout when large offset-to-depth ratios are combined with high levels of anellipticity, as indicated by (b).

Clearly, the ATT approximation allows accurate flattening up to extreme levels of anellipticity for $x/z \leq 2$, albeit with biased estimates of the anisotropy parameters (see Figure 2), but loses accuracy with increasing x/z. The effective rational interpolation provides better accuracy than the ATT approximation but shows a small amount of residual moveout as the level of anellipticity becomes high to extreme. This indicates that treating intervals composed of layers with high levels of anellipticity as a single effective layer could lead to somewhat biased effective estimates and inaccurate flattening of the moveout. When such incorrect flattening is observed, these intervals could be divided into smaller ones. Finally, Figure 4c depicts the ability of our method to flatten the events accurately up to extreme levels of anellipticity and large x/z.

To estimate the robustness of the method in the presence of noise, we evaluated it in the presence of two different types of noise. First, we applied uncorrelated random time shifts to each individual trace in Figure 1 to simulate the presence of statics. A series of tests were performed where the maximum absolute static shift applied increased from 1 to 18 ms. The dominant period of the events was about 50 ms; thus, in the extreme cases there could be jumps in traveltime of more than half a dominant period. The latter can be considered large static shifts.

We first created an ensemble of 50 gathers with different realizations of random static shifts for each test. We then calculated the average values as well as the standard deviations of the estimated parameters V_{nmo}, V_{hor}, and η and plotted them as a function of the maximum absolute value of the static shifts in Figure 5. We analyzed the data using both the GT method (Figure 5a) and our method (Figure 5b). The drawn lines are the obtained averages, and the dashed lines represent the true parameter values. The shaded areas indicate the obtained parameter averages plus or minus one standard deviation. The green curves are related to the parameters for the first layer, and the blue, red, and cyan curves are related to the second to fourth layers, respectively. The analysis is done for a maximum x/z ratio of 2.5. This is often quoted as the maximum x/z ratio in practical acquisition design, and it is usually regarded as the minimum x/z value needed for robust interval parameter estimation.

Clearly, our method is stable and has a negligible systematic error in the presence of random static shifts for arbitrary levels of anellipticity. The GT method is without such systematic error for relatively small values of anellipticity only. This leads to biased parameter estimates for higher levels of anellipticity, just as in the noise-free case (see Figure 2). Furthermore, the error bars for V_{hor} (and thus η) in our method are smaller for all layers than the respective error bars for the GT method except for the first (elliptical) layer, with the largest differences occurring for the layers with highest anellipticity (i.e., layers three and four). This is a direct result of the improved accuracy of the traveltime curves obtained with our method for higher levels of anellipticity and larger offsets. For the maximum x/z ratio of 2.5, the improvement is indeed most significant for larger levels of anellipticy (see Figure 4). For the first elliptical layer, the error bars for both methods are about the same size because in this case the GT method is exact.

We mention that the error bars for the estimates of V_{hor} (and thus η) for the third layer are substantially smaller than for the other layers. This can be explained by observing that, for this layer, V_{hor} is apparently better resolved than for the other layers, as is evident from the more horizontal character of the semblance contours for this layer in Figure 1. The general observed robustness of our method in the presence of noise is confirmed for x/z values up to four. The maxi-

mum-semblance values obviously deteriorate with increasing values of maximum absolute static shifts for both methods. The results remain stable for shifts up to ± 10 ms approximately (Figure 5).

The second type of noise we considered was uniformly distributed random noise added to the noise-free data in Figure 1 with varying signal-to-noise (S/N) ratios. Here, the S/N ratio is defined as the maximum sample value of all traces in the gather divided by the average power of the noise. The added noise had the same bandwidth as the signal. Figure 6 shows four realizations of noise added to the noise-free data of Figure 1 with varying S/N ratios. Just as in Figures 5 and 7, we plot the estimated values of V_{nmo}, V_{hor}, and η for both methods but as a function of the S/N ratio. The analysis was here for a maximum x/z ratio of 2.5.

Our method remained robust and without systematic error for arbitrary levels of anellipticity up to small S/N ratios, whereas the GT method did so for relatively small levels of anellipticity only. Just as in the case of the random static shifts, our method had overall smaller error bars for V_{hor} (and thus η) than the GT method. This behavior was confirmed for x/z values up to four. With both different types of noise, the error bars for η were always larger than the error bars for V_{nmo} and V_{hor}. Indeed, the statement from Grechka and Tsvankin (1998, p. 996) that the "corresponding absolute change in the parameter η is at least as large as the sum of the relative changes in V_{nmo} and V_{hor}" was satisfied.

Both noise tests confirmed that rational-interpolation semblance analysis leads to more accurate interval velocity and anisotropy estimates than the conventional GT technique and remains robust in the presence of moderate statics and/or noise-contaminated data.

DISCUSSION

The accuracy of any inversion of the moveout for the anisotropy parameters in TI media is hampered by the inherent trade-off relations between the relevant parameters V_{nmo} and V_{hor}. This is pointed out by Grechka and Tsvankin (1998), who show that exact ray-tracing of models with η values as different as 0.09 and 0.24 have maximum traveltime differences of about 3 ms only for x/z ratios up to two (see their Figures 2 and 3). Thus, the inversion for η is inherently uncertain and more sensitive to the presence of noise. This is evident from the size of the error bars in Figures 5 and 7 for η when compared to the error bars for V_{nmo} and V_{hor}. However, the trade-off relation becomes less severe for increasing x/z ratios, as is evident from our Figure 3 and as pointed out by Alkhalifah (1997), Grechka and Tsvankin (1998), Wookey et al. (2002), and Douma and Calvert (2006). This provides an incentive to devise a method that is accurate up to large x/z ratios, such as ours.

It is known that rational interpolation can be accompanied with the presence of unwanted poles. Such poles occur when the numerator is nonzero but the denominator becomes zero (or close to zero) away from the support offsets x_i. This is different from the above-mentioned degeneracy because then both the numerator and denominator are zero. In the presence of poles, the interpolated moveout curve shows a large oscillation between two support points. After the reciprocal differences in the Thiele continued fraction are calculated, however, the presence of poles can easily be verified by checking for zeroes in the denominator not accompanied by zeroes in the numerator of the rational approximation. Such poles should be well away from the real axis and the interval between the first and last support offset (Figure 8). This can be understood by realizing that the presence of a pole close to the real axis would be observable on the real axis through inaccurate interpolation of the traveltime between the support offsets.

We have not tested the extent of this pole-free area (Figure 8). In case this area does contain poles, one can try choosing different support points for the interpolation. Considering that such poles will occur only sporadically, however, the semblance calculation for this

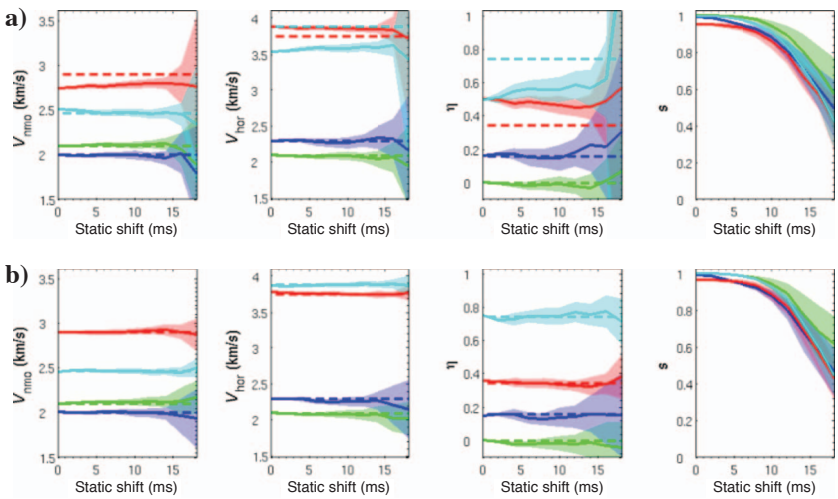

Figure 5. Sensitivity of both (a) the GT method and (b) our method to the presence of random static shifts. Average estimates of V_{nmo}, V_{hor} and η, as well as the average accompanied maximum semblance value s, are shown by the lines drawn for layers 1 (green), 2 (blue), 3 (red), and 4 (cyan). The shaded areas indicate the estimated averages plus or minus one standard deviation, and dashed lines are the true values of V_{nmo}, V_{hor}, and η. Our method is robust and with negligible systematic error for arbitrary levels of anellipticity, whereas the GT method is unbiased for relatively small levels of anellipticity only. The rational interpolation method has overall smaller error bars and is robust in the presence of larger static shifts than the GT method.

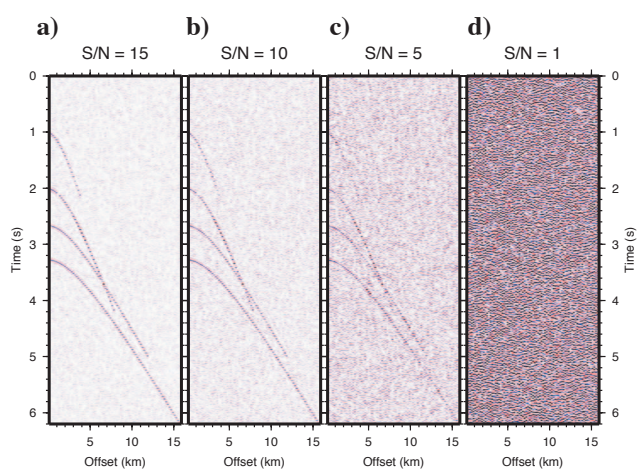

Figure 6. Examples of single realizations of noise added to the noise-free data of Figure 1 with differing S/N ratios.

particular combination of V_{nmo} and V_{hor} can be skipped altogether and found from interpolating neighboring semblance estimates (i.e., from the semblances obtained using neighboring values of V_{nmo} and V_{hor} in the semblance scan).

In the limit of infinite offset, the [2/2] rational interpolant converges to $\lim_{X\to\infty} T(X) = T_0$. This causes the interpolant in equation 8 to oscillate with large amplitudes beyond the maximum support offset. The condition generally holds for $[L/M]$ rational interpolation where $L = M$ — hence, the remark made by Douma and Calvert (2006) that extrapolation beyond the largest support offset should in general be avoided, as we do in this work. Moveout should become linear at large offset-to-depth ratios. Using a $[M + 1, M]$ scheme, the limit of the interpolant indeed becomes linear, i.e., $\lim_{X\to\infty} T(X) = (n_M + n_{M+1}X)/d_M$. Such a scheme would potentially allow some extrapolation beyond the maximum support offset. The maximum support offset where high accuracy is still obtained is of course a direct function of the order of the interpolation: a higher order means better accuracy at larger x/z ratios. Thus, by increasing the order of the interpolation, the method can be tuned to be accurate at arbitrary x/z ratios.

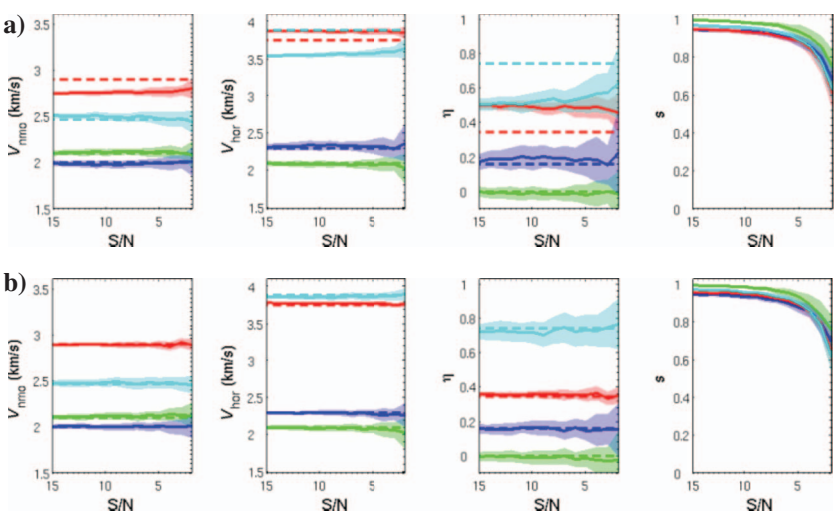

Figure 7. Same as Figure 5 but now as a function of the S/N ratio. Our method is robust and without systematic error up to small S/N ratios for arbitrary levels of anellipticity, whereas the GT method leads to unbiased results for relatively small levels of anellipticity only. Overall, our method has smaller error bars than the GT method and remains robust and unbiased up to smaller S/N ratios. Maximum semblance values are again stable for a large range of S/N ratios.

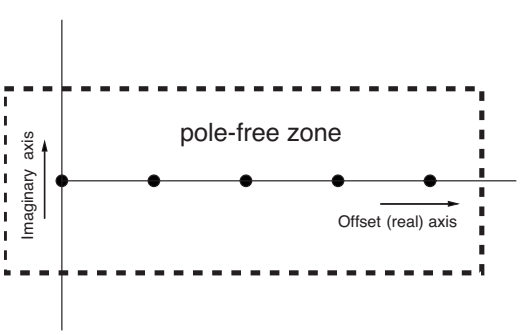

Figure 8. Sketch showing the area near the (real) offset axis that should be without poles for the rational interpolation to be accurate. The black dots are the support offsets for the interpolation.

Our method requires calculating only a few support points to obtain accurate traveltime curves as a function of offset for qP-waves in horizontally layered VTI media. Although we show its accuracy only in the context of moveout analysis, it seems worthwhile to investigate the use of rational interpolation in more general traveltime calculations such as prestack time migration in VTI media or even in the context of sparse storage of traveltimes. Sparse storage is relevant in everyday seismic data processing where large traveltime tables are used for imaging and inversion. The method presented here is, of course, directly applicable to the problem of Kirchhoff time migration in layered VTI media.

Other authors seem to have been inspired by our interpolation approach and have also abandoned the approximation route in favor of an interpolation approach. Of course, any interpolant that is well adapted to describing qP-wave moveout in layered VTI media is suited. In this context, we mention the Hermite interpolation approach of Fomel and Stovas (2007). It achieves an accurate approximation for reflection moveout in layered media given only a single nonzero-offset ray.

In principle, the method can also be extended to handle qP-waves in azimuthally anisotropic media, e.g., transversely isotropic areas with a horizontal symmetry axis (HTI), or to deal with converted waves in both VTI and HTI media. See Van der Baan and Kendall (2003) for the relevant expressions. Naturally, this increases the number of anisotropy parameters involved and renders the rational interpolation and subsequent semblance analysis less straightforward to implement. For all these possible extensions, it is implicitly assumed that a rational approximation provides reasonable but not accurate enough traveltimes. This justifies its replacement with an interpolant with the same functional dependence, i.e., a rational one, as done here for VTI anisotropy.

Finally, a note of caution: The developed semblance-based inversion method is accurate at arbitrary large offset-to-depth ratios and in the presence of large anistropy. However, it assumed that no lateral velocity and/or anisotropy variations occur. This is a fundamental restriction underlying all inversion methods based on a 1D, layered-earth assumption. A full tomographic approach is required if strong lateral velocity variations are anticipated. Our approach can still be used to infer NMO velocities and anisotropy parameters suitable for an initial model estimate if a full tomographic approach is required.

CONCLUSION

The τ-p domain is the natural domain for anisotropy parameter estimation in horizontally layered media. It leads to more accurate anisotropy parameter estimates and accounts for ray bending caused by horizontal layering. But τ-p methods need to either transform the data to the τ-p domain or pick traveltimes in the t-x domain, both of which are practical disadvantages. To overcome this, we combine τ-p-derived traveltimes and offsets with a rational interpolation procedure applied in the t-x domain. We thus devise a semblance-based approach in the t-x domain that allows accurate and robust interval

anisotropy parameter estimation. This extends the approach of Douma and Calvert (2006), valid for nonhyperbolic-moveout inversion of qP-waves in a single horizontal VTI layer, to the case of horizontally layered VTI media.

The method is accurate and efficient because rational interpolation produces accurate traveltime predictions given only few support points. These support points are in turn calculated efficiently using the derived τ-p expressions for the traveltimes and associated offsets. The resulting inversion method is accurate at arbitrarily large offset-to-depth ratios, making it particularly attractive for shallow targets where such large ratios are easily encountered in practice. Our method allows the computation of semblance scans as a function of interval horizontal and NMO velocities when it is applied in a layer-stripping fashion.

Synthetic data examples confirm the accuracy of the predicted moveout curves and the resulting unbiased interval velocity and anisotropy estimates after a semblance analysis. Our method is shown to be robust in the presence of noise in the form of both random static shifts and random added noise.

ACKNOWLEDGMENTS

The anisotropic ray tracing used to calculate the traveltimes for the events in the CMP gather of Figure 1a was done using the ANRAY ray-tracing package from the Seismic Waves in Complex 3D Structures (SW3D) consortium project at Charles University in Prague. The suggestions of Sergey Fomel, Vladimir Grechka, Ivan Vasconcelos, and two anonymous reviewers are much appreciated and helped improve the manuscript. Several illustrations in this work were obtained using Generic Mapping Tools (Wessel and Smith, 1998). This work was supported by the sponsors of the Consortium Project on Seismic Inverse Methods for Complex Structures at the Center for Wave Phenomena and by National Science Foundation grant DMS-0530865.

APPENDIX A

DEGENERACY OF [2/2] RATIONAL INTERPOLATION FOR HYPERBOLIC MOVEOUT WHEN SQUARED OFFSETS AND SQUARED TRAVELTIMES ARE INTERPOLATED

To show that the linear system in equation 10 becomes degenerate for purely hyperbolic moveout when squared offset and squared traveltime are interpolated, we first set $L = M = 2$ in equation 8. This gives us

$$T(X) \approx \frac{T_0 + n_1 X + n_2 X^2}{1 + d_1 X + d_2 X^2}, \tag{A-1}$$

where we use $n_0 = T_0$ with T_0 the squared zero-offset two-way traveltime. Rewriting equation A-1 into the form of equation 10 and using four support points (X_i, T_i), we arrive at a linear system of equations for the unknown interpolation coefficients n_1, n_2, d_1, d_2, i.e.,

$$A \cdot \mathbf{x} = \mathbf{d}, \tag{A-2}$$

where

$$A := \begin{pmatrix} -X_1 & -X_1^2 & X_1T_1 & X_1^2T_1 \\ -X_2 & -X_2^2 & X_2T_2 & X_2^2T_2 \\ -X_3 & -X_3^2 & X_3T_3 & X_3^2T_3 \\ -X_4 & -X_4^2 & X_4T_4 & X_4^2T_4 \end{pmatrix}, \tag{A-3}$$

$$\mathbf{x} := \begin{pmatrix} n_1 \\ n_2 \\ d_1 \\ d_2 \end{pmatrix}, \quad \mathbf{d} := \begin{pmatrix} T_0 - T_1 \\ T_0 - T_2 \\ T_0 - T_3 \\ T_0 - T_4 \end{pmatrix},$$

with T_0 the squared two-way zero-offset traveltime. Calculating det A, we get

$$\begin{aligned} \det A = {} & X_1X_2X_3X_4[(T_1T_2 + T_3T_4)(X_1 - X_2)(X_3 - X_4) \\ & + (T_1T_4 + T_2T_3)(X_2 - X_3)(X_1 - X_4) \\ & - (T_1T_3 + T_2T_4)(X_1 - X_3)(X_2 - X_4)]. \end{aligned} \tag{A-4}$$

When the moveout is purely hyperbolic, $T_i = T_0 + X_i/v^2$ and thus

$$X_i - X_j = v^2(T_i - T_j). \tag{A-5}$$

Inserting equation A-5 into equation A-4 gives

$$\begin{aligned} \det A = {} & v^2X_1X_2X_3X_4[(T_1T_2 + T_3T_4)(T_1T_3 - T_1T_4 - T_2T_3 \\ & + T_2T_4) + (T_1T_4 + T_2T_3)(T_1T_2 - T_2T_4 - T_1T_3 \\ & + T_3T_4) - (T_1T_3 + T_2T_4)(T_1T_2 - T_1T_4 - T_2T_3 \\ & + T_3T_4)] \end{aligned} \tag{A-6}$$

$$\begin{aligned} = {} & v^2X_1X_2X_3X_4[(T_1T_2 + T_3T_4)(T_1T_3 - T_1T_4 - T_2T_3 \\ & + T_2T_4) - (T_1T_2 + T_3T_4)(T_1T_3 - T_1T_4 - T_2T_3 \\ & + T_2T_4) + (T_1T_3 + T_2T_4)(T_1T_4 + T_2T_3) \\ & - (T_1T_3 + T_2T_4)(T_1T_4 + T_2T_3)] \end{aligned} \tag{A-7}$$

$$= 0. \tag{A-8}$$

Therefore, for hyperbolic moveout, the linear system 10 for [2/2] rational interpolation of the moveout, expressed as squared traveltime as a function of squared offset, is degenerate.

REFERENCES

Alkhalifah, T., 1997, Velocity analysis using nonhyperbolic moveout in transversely isotropic media: Geophysics, **62**, 1839–1854.
———, 1998, Acoustic approximations for processing in transversely isotropic media: Geophysics, **63**, 623–631.
———, 2000, The offset-midpoint traveltime pyramid in transversely isotropic media: Geophysics, **65**, 1316–1325.
Alkhalifah, T., and M. de Hoop, 2005, Residual dip moveout in VTI media: Geophysical Prospecting, **53**, 1–12.
Alkhalifah, T., and I. Tsvankin, 1995, Velocity analysis for transversely isotropic media: Geophysics, **60**, 1550–1566.
Alkhalifah, T., I. Tsvankin, K. Larner, and J. Toldi, 1996, Velocity analysis and imaging in transversely isotropic media: Methodology and a case study: The Leading Edge, **15**, 371–378.
Dix, C., 1955, Seismic velocities from surface measurements: Geophysics, **20**, 68–86.
Douma, H., and A. Calvert, 2006, Nonhyperbolic moveout analysis in VTI

media using rational interpolation: Geophysics, **71**, no. 3, D59–D71.
Fomel, S., 2004, On anelliptic approximations for qP velocities in VTI media: Geophysical Prospecting, **52**, 247–259.
Fomel, S., and A. M. Stovas, 2007, Generalized non-hyperbolic moveout approximation: 69th annual meeting, EAGE, Extended Abstracts, B041.
Grechka, V., and I. Tsvankin, 1998, Feasibility of nonhyperbolic moveout inversion in transversely isotropic media: Geophysics, **63**, 957–969.
Hake, H., 1986, Slant stacking and its significance for anisotropy: Geophysical Prospecting, **34**, 595–608.
Hake, H., K. Helbig, and C. Mesdag, 1984, Three-term Taylor series for t^2-x^2 curves over layered transversely isotropic ground: Geophysical Prospecting, **32**, 828–850.
Sarkar, D., R. Baumel, and K. Larner, 2002, Velocity analysis in the presence of amplitude variation: Geophysics, **67**, 1664–1672.
Stoer, J., and R. Bulirsch, 1993, Introduction to numerical analysis: Springer-Verlag, 2nd edition.
Stovas, A., and B. Ursin, 2004, New traveltime approximations for a transversely isotropic medium: Journal of Geophysics and Engineering, **1**, 128–133.
Thomsen, L., 1986, Weak elastic anisotropy: Geophysics, **51**, 1954–1966.
Tsvankin, I., 1996, P-wave signatures and notation for transversely isotropic media: An overview: Geophysics, **61**, 467–483.
Tsvankin, I., and L. Thomsen, 1994, Nonhyperbolic reflection moveout in anisotropic media: Geophysics, **59**, 1290–1304.
Ursin, B., and A. Stovas, 2006, Traveltime approximations for a layered transversely isotropic medium: Geophysics, **71**, no. 2, D23–D33.
Van der Baan, M., 2004, Processing of anisotropic data in the τ-p domain: I — Geometric spreading and moveout corrections: Geophysics, **69**, 719–730.
Van der Baan, M., and J. M. Kendall, 2002, Estimating anisotropy parameters and traveltimes in the τ-p domain: Geophysics, **67**, 1076–1086.
——–, 2003, Traveltime and conversion-point computations and parameter estimation in layered, anisotropic media by τ-p transform: Geophysics, **68**, 210–224.
Wessel, P., and W. Smith, 1998, New, improved version of generic mapping tools released: EOS Transactions of the American Geophysical Union, **79**, 579.
Wookey, J., M. Van der Baan, D. Smit, and J.-M.Kendall, 2002, Tau-p domain VTI parameter inversions using limited-offset data: 64th Meeting, EAGE, Extended Abstracts, F041.
Zhang, F., and N. Uren, 2001, Approximate explicit ray velocity functions and traveltimes for P-waves in TI media: 71st Annual International Meeting, SEG, Expanded Abstracts, 106–109.